Cerâmica. 2024, v.70:eWKZU9068 http://dx.doi.org/10.1590/WKZU9068
ORIGINAL ARTICLE

Adsorption of methylene blue dye on construction and demolition waste in an aqueous medium

H. J. B. da Silva[1]*, M. L. de Sá[1], R. S. de Oliveira[2], M. R. M. C. Santos[1], J. M. E. de Matos[1]
[1]Federal University of Piauí, Interdisciplinary Laboratory of Advanced Materials, 64049-550, Teresina, PI, Brazil
[2]Federal University of Pernambuco, Department of Production Engineering, 50670-901, Recife, PE, Brazil

Abstract

The present research proposed the use of construction and demolition waste (CDW) in adsorption of methylene blue dye in aqueous medium. CDW was studied in its natural form and calcined aiming to improve its properties, both being characterized by different techniques and subjected to adsorption studies. From the kinetic study, it was verified that both systems presented a better fit to the experimental data for the pseudo-second-order model (R^2 >0.980). The concentration and temperature variation showed a maximum adsorption capacity of 112.23 $mg.g^{-1}$ (natural) and 418.6 $mg.g^{-1}$ (calcined) both for the temperature of 45 ºC. The experimental data fit better with the Langmuir isotherm model, with a correlation coefficient R^2 ≥0.960 for both samples. It was observed that both residues presented favorable adsorption mechanisms and effective adsorption parameters, but the calcined sample presented better results, and thinking in a low-cost material, natural sample can be more economically advantageous. In this view, CDW represents a potential and promising alternative for water purification.
Keywords: adsorption, methylene blue dye, construction and demolition waste.

INTRODUCTION

In recent years, many discussions have been made around the environmental issue, and topics related to solid waste management, environmental preservation, and recycling have gained prominence and great importance among researchers, especially to seek solutions to the problems that arise as a result of the constant transformations of ecosystems in the function of human action to achieve a model of sustainable development for the planet [1, 2]. Minimizing the environmental impacts caused by the disposal of chemicals in nature is a major concern that permeates sustainable development, and therefore several studies have been conducted to reduce these impacts through alternatives that do not harm but are beneficial to the environment, such as is the case of the treatment of artificial dyes widely used by industries [3]. When it comes to the textile sector, it is known that its main characteristic is the high consumption of water, as well as the generation of solid waste, atmospheric emissions, and effluents that are harmful to the environment [4]. The water used in washing and dyeing processes carries residues of dyes that are discarded in nature through textile effluents [5]. Around 10,000 types of synthetic dyes are used by the textile and dye industry, and for some types of dyes, 50% of the used does not attach to tissue fibers, leading to the formation of wastewater [6, 7].

Among the various dyes used in the dyeing process of cotton, wood and leather, besides being used also by the pharmaceutical industry, we can highlight the synthetic methylene blue dye, one of the contaminants of water bodies best known for causing problems in the environment, because it blocks the entry of sunlight into aquatic environments, hindering the photosynthesis process and threatening the life of organisms that inhabit in this environment. In addition, it can also cause health problems such as abdominal disorders, difficulty breathing, skin sensitivity and blindness [8] and aquatic biota by reducing water oxygen levels, affecting plant photosynthesis, leading to suffocation of aquatic flora and fauna [9-11]. The removal of methylene blue dye from wastewater is vitally important, because even in a small amount, it can cause damage to nature. Currently, there are several techniques used for the removal of dyes from industrial effluents, such as coagulation, filtration, ion exchange, biological treatment, advanced oxidation processes, electrolysis, among others [12]. Nevertheless, much has been researched about increasingly effective methods for the treatment of dyes, especially capable of aligning efficiency and low cost [13]. However, among the possibilities existing for this purpose, adsorption stands out, as the most used treatment process, because it is very effective, simple and economical. It consists of the interaction between the outer surface of an adsorbent and an adsorbate, through the adsorbate particles on the adsorbent surface. The adsorption process depends on several factors such as the initial level of pollutants, the pH of the solution, adsorbent dosage, mixing rate and temperature [14]. In recent years, the search for complementary or alternative techniques for the removal of pollutants from the water system with minimal impact on the environment has been a topic of great interest to science [15]. Therefore, it is necessary to encourage the use of alternative materials, to the detriment of consecrated materials, but of high purchasing value, thus enabling more attractive costs and good results [16]. On the other hand, the

**hitalo.ufpi@gmail.com*
https://orcid.org/0000-0001-6008-3600

study of a specific contaminant, such as methylene blue dye, is important because it helps to understand the mechanisms of interaction of adsorbent, as well as evaluate its efficiency and improve the remotion conditions. These studies permit the development of experimental protocols, establishment of reference parameters and evaluations of the selectivity and capacity of adsorbent regeneration. Moreover, the information gained from these studies can be extrapolated to more complex wastewater systems, providing important insights and guidelines for dye removal in realistic conditions.

Parallel to the problem of wastewater treatment containing the methylene blue dye, widely used for tissue dyeing, the management of construction and demolition waste (CDW) is a major challenge to be overcome by the construction industry and the municipal government due to the high volume generated from construction and demolition activities, as well as the impact that this material generates on the environment. In Brazil, the mineral CDW from constructions and demolitions is mixed and variable, and presents in its composition three basic mineral materials, mostly concrete/mortars, ceramics and rocks, but may also present fractions of plastics, paper, wood, bituminous materials, among others, including hazardous waste, depending on the origin of this waste [17-19]. Considered one of the largest waste streams in the world, the CDW corresponds to 30-40% of the total solid waste due to large-scale construction and demolition activities resulting from rampant urban development. Therefore, this rapid urbanization is not only responsible for increasing the consumption of natural resources, but also for the generation of large amounts of waste, which contribute to increased pollution, resource depletion and land deterioration, and because there is no adequate waste management plan, the CDW generated is simply dumped or used in landfills [18, 19]. After water, concrete is the second most consumed material in the world, and its high consumption is closely related to current urban development, as concrete is used twice as much as the sum of all other building materials [20]. Moreover, as we know, the construction industry has been growing rapidly in recent decades and, with this, there has also been a lot of rubble, and high costs to municipalities regarding the management of these materials [21].

Many studies on the impacts related to CDW management strategies have been conducted, and most of them are perceived as adopting the life cycle assessment methodology [22-25]. Thinking about sustainable development and cost reduction, it is possible to combine the constant generation of construction and demolition waste as an alternative material applied to the treatment of effluents containing the synthetic methylene blue dye. Reviewing the available literature, it was noticed that studies involving low-cost alternative materials have been widely carried out, even residues of ceramic materials have been successfully used, however, studies involving the use of CDW, which includes, in addition to red ceramic residues, cementitious residues and rocks, have not yet been used as alternative and low-cost materials applied to the adsorption of methylene blue dye. The high availability and low cost of this residue would make it an adsorbent with great application potential in adsorption, and in contrast, would contribute to the proper management of urban waste. The advantages provided by the recycling and reuse of these wastes as alternative adsorbents are interesting to environmental and economic aspects, since, in addition to the reduction of costs in terms of the treatment of these materials by the public authorities, it represents a raw material with interesting properties, at a low cost, being, therefore, much cheaper than the natural aggregate [26]. From this perspective, the present research aimed to apply construction and demolition waste in the process of adsorption of methylene blue dye. Therefore, to optimize results, it was carried out a calcination treatment of the natural CDW and the results were compared. However, it was observed that despite the treatment of calcination can provide better adsorption results, it involves costs, making the adsorption process more expensive, so that the use of natural sample can be more economically advantageous.

MATERIALS AND METHODS

Construction and demolition waste: the CDW used came from several civil construction works in the city of Teresina-PI, Brazil, and was therefore collected manually, and packed in nylon bags. The collected waste consisted mainly of red ceramics (bricks and tiles), ceramic coating, mortar residue, concrete and pebble. It was crushed in a jaw crusher (Metso) and then manually sifted in an ASTM 120 mesh/Tyler granulometric sieve, opening 125 μm.

Thermal treatment method of CDW: the sifted CDW was calcined to improve its natural properties for application in the adsorption process. For this, a sample of CDW was calcined in a muffle oven (10P-S, EDG). The firing parameters were: heating and cooling rate at 10 ºC.min^{-1}, at 700 ºC for 2 h [27]. After calcination, the sample was macerated and declustered in a crucible, and then sieved in a sieve of 125 μm of opening.

Methylene blue dye: as a product widely used in the textile industry, methylene blue dye is commonly the target of effluent treatment studies of this type of manufacture [28]. The product used (Dinâmica Quím. Contemp.) had chemical composition $C_{16}H_{18}ClN_3S.3H_2O$, with molecular weight of 373.90 g.mol^{-1}, and 97% of purity. Chemical structure of methylene blue dye is shown in Fig. 1.

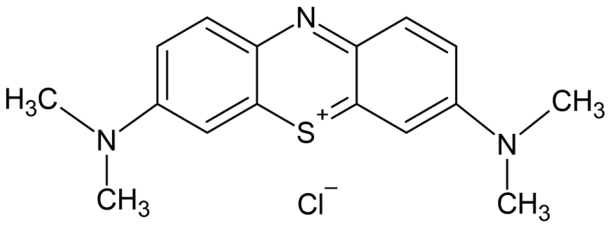

Figure 1: Chemical structure of methylene blue dye.

Characterization techniques: the analyses of the crystallographic profiles of the samples were determined by the X-ray diffraction technique (XRD), performed with a diffractometer (Multiflex, Rigaku) using CuKα radiation, in the range of 2θ from 10° to 80° and speed of 2 °.min^{-1}. Fourier-transform infrared spectroscopy (FTIR) analyses were performed in a spectrophotometer (Spectrum 100, PerkinElmer) with scanning range between 400 and 4000 cm^{-1}, performing 16 scans with resolution of 4 cm^{-1}. Thermal analyses were carried out with an equipment (Q600 SDT, TA Instr.) with temperature variation between 10 and 1000 ºC, and heating rate of 10 ºC.min^{-1}. X-ray fluorescence spectroscopy (XRF) of the samples was performed with a spectrometer (Epsilon 3-XL/30, Panalytical). The characterization of the surface morphology of the samples was determined by field emission-scanning electron microscopy (FE-SEM), performed with a microscope (JSM 7500F, Jeol). To determine the surface area and pore volume of the samples, the technique of adsorption and desorption of nitrogen - Brunauer, Emmett and Teller (BET) was used with an analyzer (2200 E, Nova Instr.). The concentration of methylene blue dye was determined by ultraviolet-visible spectrophotometer (UV-vis, 60 UV-VIS, Cary) at wavelength λ=665 nm.

Point of zero charge (pH_{pzc}): the point of zero charge of the samples were determined by the solid addition method, in which 10 mg of each sample was placed in polyethylene tubes, in which 20 mL of KNO_3 at 0.1 mol.L^{-1} with initial pH (pH_i) adjusted with the aid of NaOH and HCl at 0.1 mol.L^{-1}, ranging from 2 to 12. The tubes were placed in constant agitation at 180 rpm for 24 h. At the end of this period, the tubes were centrifuged, and the final pH (pH_f) was measured. The pH_{pzc} corresponded to the range where the pH of the solution remained constant, that is, where the pH variation (pH_i–pH_f) was equal to zero [29-31].

Adsorption studies of methylene blue dye: tests were carried out to determine the adsorptive properties of the adsorbent/adsorbate interface. Therefore, the effects of adsorbent dosage, pH, contact time, temperature and adsorbate concentration were analyzed. All studies were performed in triplicate. *Effect of adsorbent dosage*: a solution with a concentration of 100 mg.L^{-1} of methylene blue dye in ultrapure deionized water was used. In addition, 10, 20, 30, 40, 50 and 100 mg of the natural and calcined residues were weighed, then being put in contact with 20 mL of dye solutions in polyethylene tubes, subjected to agitation at 180 rpm for 24 h at 25.0±1.0 ºC. Then, the samples were centrifuged at 5000 rpm for 20 min, and the concentration of the supernatant was determined by UV-vis spectroscopy. The adsorption capacity can be calculated by Eq. A, based on the mass balance [32]:

$$q_e = \frac{(C_i - C_f).V}{m} \quad (A)$$

in which: q (mg.g^{-1}) is the amount adsorbed per gram of adsorbent; C_i is the initial concentration of the solute (mg.L^{-1}); C_f is the final concentration of adsorbate (mg.L^{-1}); V (L) is the volume of the solution; m (g) is the mass of the adsorbent. *Effect of pH*: methylene blue dye solutions were used for the pH study at 100 mg.L^{-1}, so that dye solutions were calibrated with pH ranging from 2 to 12. Thus, the residue (natural and calcined) doses determined in the dosage study were immersed in 20 mL of dye solution at the various pH values, and submitted to constant agitation at 180 rpm for 24 h at 25.0±1.0 ºC. At the end, the samples were centrifuged to separate the phases, and the concentration of the supernatant was determined by UV-vis spectroscopy. *Effect of contact time*: the effect of contact time between the samples of natural and calcined residues with the dye solution was performed taking into account the masses of the materials determined by the dosage study, and also in observance of the pH that most favored the adsorption of the dye by the samples. In this sense, the determined masses of each sample were immersed in 20 mL of dye solution contained in polyethylene tubes, left under constant agitation at 180 rpm ranging from 60 to 1440 min at 25.0±1.0 ºC. Then, the samples were centrifuged to separate the phases, and the concentration of the supernatant was determined by UV-vis spectroscopy. Thus, the kinetic models were used to predict the kinetic constants of adsorption [33, 34]. To evaluate the adsorption kinetics of adsorbent/adsorbate systems, the experimental data were adjusted to the pseudo-first-order, pseudo-second-order and Elovich model, represented by the Eqs. B, C, and D, respectively:

$$\ln(q_{e,exp} - q_t) = \ln q_{e,cal} - k_1.t \quad (B)$$

$$\frac{t}{q_t} = \frac{1}{k_2 q_{e,cal}^2} + \frac{1}{q_{e,cal}} t \quad (C)$$

$$q_t = \frac{1}{\beta} \ln(\alpha.\beta) + \frac{1}{\beta} \ln t \quad (D)$$

where $q_{e,exp}$ and $q_{e,cal}$ (mg.g^{-1}) represent the amount adsorbed per gram of adsorbent, q_t (mg.g^{-1}) refers to the amount adsorbed per gram of adsorbent in time t (min), k_1 (min^{-1}) is the pseudo-first-order velocity constant, k_2 (g.mg^{-1}.min^{-1}) is the pseudo-second-order velocity constant, β (g.mg^{-1}) is the adsorption constant, being related to the degree of coverage of the adsorbent surface and the activation energy of the chemisorption process and α (mg.g^{-1}.min^{-1}) is initial adsorption velocity constant [35-37].

Effect of temperature and dye concentration: established the best mass, pH and contact time for both residue samples, the effects of temperature and dye concentration were studied, which took into account the variation of adsorbate concentration as well as the temperature to which the system is subjected. Thus, dye solutions were prepared at concentrations ranging from 35 to 430 mg.L^{-1}. 20 mL of each solution was separated into polyethylene tubes and the respective quantities of mass previously determined for the natural and calcined samples

were added, and then submitted to constant agitation of 180 rpm at 25, 35 e 45 °C, for a previously determined time in the kinetic study. At the end of agitation, the tubes were centrifuged at 5000 rpm for 10 min to separate the phases and the concentration of supernatant was determined by UV-vis spectroscopy. All experiments were carried out in triplicate. Thus, the experimental data obtained from the tests were later adjusted to the physical-chemical models proposed by Langmuir, Freundlich and Temkin [38, 39]. With the linearization of the equations by the obtained data, it was possible to determine the theoretical adsorption isotherms and compare them to the values found experimentally. The model proposed by Langmuir is described by the occurrence and monolayers in homogeneous sites of the adsorbent, and is described by [40]:

$$q_e = \frac{K_L.q_m.C_e}{1+K_L.C_e} \quad (E)$$

where q_m ($mg.g^{-1}$) is the maximum adsorption capacity for monolayer formation, C_e ($mg.L^{-1}$) is the adsorbate concentration at equilibrium, K_L is the Langmuir's adsorption constant and q_e ($mg.g^{-1}$) is the adsorption capacity at equilibrium. The isotherm model described by Freundlich considers a heterogeneous adsorption surface, with multilayer formation, and does not presuppose saturation of the adsorbent surface, assuming that the concentration of adsorbate on the adsorbent surface grows infinitely as a function of adsorbate concentration [41]. The Freundlich model is described by:

$$q_e = K_F.C_e^{\frac{1}{n_F}} \quad (F)$$

where q_e ($mg.g^{-1}$) is the maximum adsorption capacity at equilibrium, C_e ($mg.L^{-1}$) is the concentration at equilibrium, K_F is the maximum adsorption capacity for the solid/liquid interface and n_F is a proportionality constant that suggests favoring or not favoring the system, that is, the affinity between adsorbent and adsorbate. The Temkin model takes into account the effects of indirect interactions between adsorbate and adsorbent on adsorption processes. Thus, reaction heats generally decrease as adsorption increases on the adsorbent surface. Isotherm is characterized by a uniform distribution of bonding energies [42]. The Temkin isotherm is given by:

$$q_e = \frac{R.T}{b} \ln (K_T.C_e) \quad (G)$$

where K_T ($L.mg^{-1}$) is the bond equilibrium constant, b is the heat adsorption, R (8.314 $J.K^{-1}.mol^{-1}$) is the universal gas constant and T is the absolute temperature (K).

Thermodynamic parameters for the adsorption: temperature is an important parameter in the adsorption process, since it involves chemical and physical transformations with energy variations to be considered. When reaching the adsorption equilibrium, it is possible to determine the thermodynamic parameters involved in the process and to weigh the results [43]. These thermodynamic parameters are the variation of Gibbs free energy (ΔG°) given in $kJ.mol^{-1}$, the variation of enthalpy (ΔH°) given in $kJ.mol^{-1}$, and the variation of adsorption entropy (ΔS°) given in $kJ.mol^{-1}.K^{-1}$. These quantities allow to determine whether the adsorption process is favorable, from the thermodynamic point of view, the spontaneity of the system, and, finally, whether the adsorption occurs with energy absorption (endothermic) or energy release (exothermic) [44]. Thermodynamic parameters intrinsic to the adsorption process can be calculated by:

$$\Delta G^o = \Delta H^o - T.\Delta S^o \quad (H)$$

$$\Delta G^o = - R.T \ln K \quad (I)$$

Combining the two equations, you have the model known as the equation of Van't Hoff:

$$\ln K = + \frac{\Delta S^o}{R} - \frac{\Delta H^o}{RT} \quad (J)$$

where R is the universal gas constant, T is the absolute temperature and K represents the adsorption equilibrium constant [45, 46]. When an adsorption process presents ΔH° negative means that this process is exothermic, that is, it releases energy in the form of heat, and involves physisorption, chemisorption or a mixture of both processes. Otherwise, if ΔH° is positive, it means to say that the process is endothermal, absorbing energy in the form of heat, and attributable to chemisorption. Negative values of ΔG° indicate that the adsorption process is pointed and favorable, on the other hand, if ΔG° is positive, the adsorption process is considered non-spontaneous and non-feasible, and in addition, a decrease in the values of ΔG° with increasing temperature indicates that adsorption is more spontaneous at higher temperatures. The magnitude and signal of ΔS° are important to verify the level of organization of the system, that is, to ΔS° negative, the organization of adsorbate in the solid/solution interface during the adsorption process becomes less random, denoting an associative mechanism, otherwise, if ΔS° is positive, then the adsorption process presents a higher degree of disorder, more random, which implies a dissociative mechanism [47].

RESULTS AND DISCUSSION

Characterization

The results of the chemical analysis of the samples are shown in Table I. The results show that the samples of natural and modified residue are predominantly composed of SiO_2 (68.23-65.29%), Al_2O_3 (13.86-14.98%), Fe_2O_3 (5.97-6.60%), and CaO (7.56-8.05%). Therefore, it can be observed the difference between natural and calcined samples was very small due to the CDW had major compound of quartz that has a high melting point and excellent thermal stability.

These results are analogue to that observed to the natural and calcined kaolin residue [48], a clay mineral that also presents a large percentage of quartz in its composition. In fact, the high percentages of silica and alumina corroborate the presence of clay minerals in the sample, as well as the proportion of Al/Si, which is commonly used as an indicator of clay permeability in relation to moisture, because they are directly proportional to each other, so that higher this proportion, greater the permeability of the material [49]. In the particular case of the materials under study, it was noted that this proportion was small, around 0.20 (natural) and 0.23 (calcined), evidencing the low level of permeability of the humidity of the samples. The percentage of mass in relation to K_2O indicated the presence of potassium feldspar (orthoclase) in the samples, whose incidence is associated with the presence of quartz. The Fe_2O_3 present in the sample is responsible for the red color after sintering [50-53].

The surface area and pore volume of the samples

Table I - Chemical analysis results (wt%) of samples obtained by XRF.

Oxide	Natural	Calcined
SiO_2	68.23	65.29
Al_2O_3	13.86	14.98
CaO	7.56	8.05
Fe_2O_3	5.97	6.60
K_2O	1.55	1.66
MgO	1.23	1.13
TiO_2	0.96	1.06
SO_3	0.49	0.57
Others	0.13	0.13

obtained by physical adsorption of N_2 are presented in Table II. It was observed that the treatment caused reduction of the surface area and a decrease of pore volume, due to the coalescence between the particles at high temperature [54]. In fact, despite the reduction of specific surface area and pore volume, the calcination can contribute to remove impurities and organic matter [55, 56] of the adsorbent and it is believed that it can make possible the interaction of charges between the CDW surface and the cationic dye.

Table II - Results obtained by physical adsorption of N_2.

Characteristic	Natural	Calcined
Specific surface area ($m^2.g^{-1}$)	9.806	4.388
Pore volume ($cm^3.g^{-1}$)	0.0039	0.0017

The XRD patterns of the samples are shown in Fig. 2. Quartz (SiO_2) was the predominant phase in all samples, due to sand particles from concrete production and also due to heating at high temperatures in the sintering of red ceramics, in which clay materials forming SiO_2 are decomposed followed by loss of its crystalline structure. A peak was observed for orthoclase, which is common in aluminosilicate with the presence of (K_2O). There was also the presence of calcite ($CaCO_3$) in the natural sample, which can be attributed to the partial carbonation of portlandite (calcium hydroxide - CaOH), because there were cement-based materials in their constitution and as observed in the decrease and disappearance of these peaks in the calcined sample, it is believed that this was due to the decomposition of the $CaCO_3$ in CaO [57]. However, due to the nature of the CDW, XRD results become complex as they associate a high number of crystalline and amorphous phases, depending on the constituents of the material (concrete, ceramic waste, mortar, sand, gravel, among others) [58].

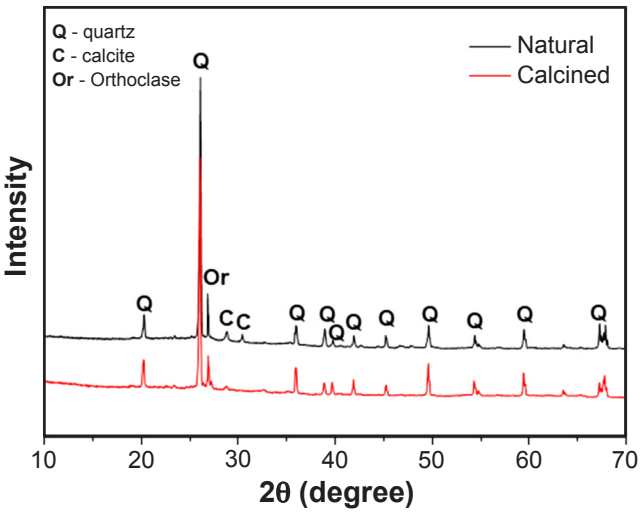

Figure 2: X-ray diffractogram of natural and calcined samples.

The FTIR spectra of the CDW samples (natural and calcined) are presented in Fig. 3. The bands around 1056, 787, and 685 cm^{-1} detected in both samples are due to Si-O and Al-O bonds commons to clay minerals, associated with the high mass percentage of these elements and the predominance of the crystalline quartz phase, as well as the band around 469 cm^{-1}, referring to vibrations Si-O-Si

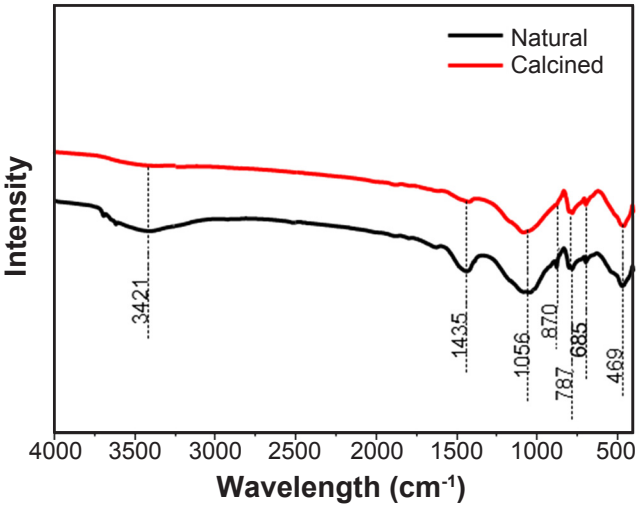

Figure 3: Fourier transform infrared spectra of natural and calcined samples.

and O-Si-O [59, 60]. The bands in 870 and 1435 cm^{-1} are characteristics of carbonates, originated by the presence of calcite in the original CDW [61]. The bands located in 3421 cm^{-1} are due to the stretch and angular vibrations of the OH group and which are related to adsorbed water and hydration water present in the material, which become more diffuse with calcination [62].

Fig. 4 presents the thermogravimetric (TG) and derivative TG (DTG) curves for natural and calcined residues. The combustion of organic matter and the loss of

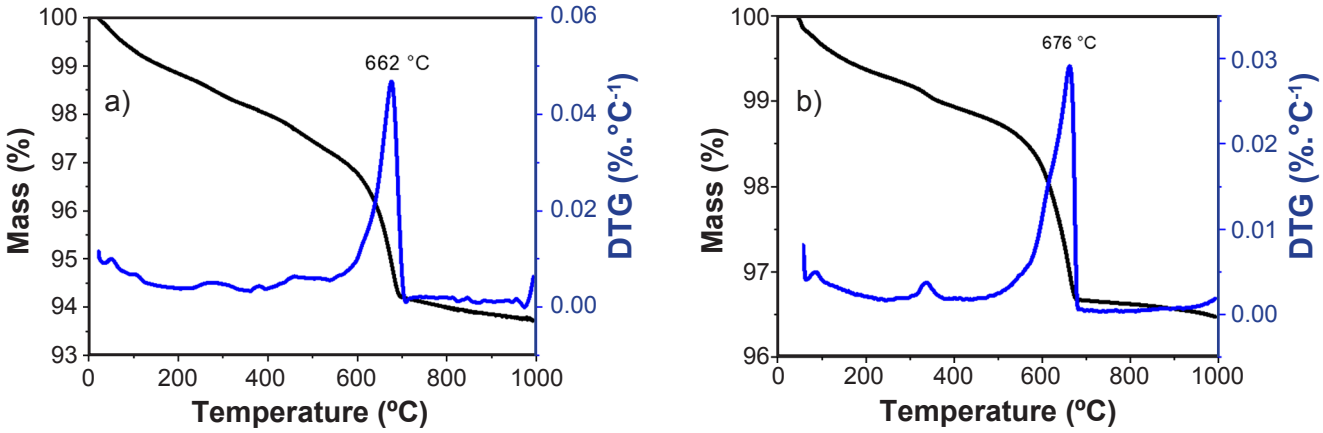

Figure 4: TG/DTG curves of natural (a) and calcined (b) samples.

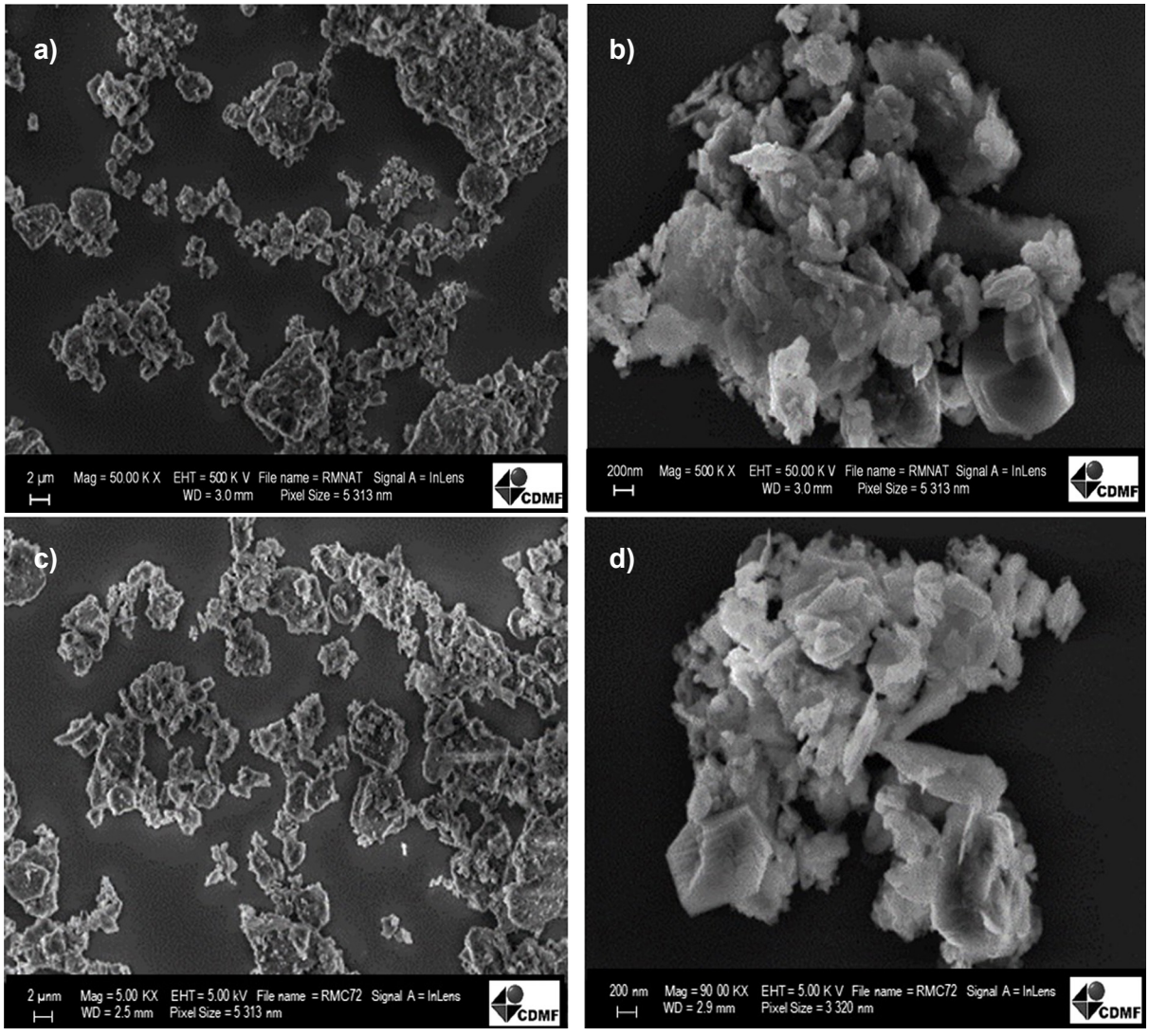

Figure 5: SEM micrographs of natural sample (a,b) and calcined sample (c,d).

adsorbed water started at low temperatures. Between 300 and 400 °C there was the loss of hydroxyls from Fe_2O_3 and Al_2O_3 chemical species. It was possible to notice a loss of gradual mass until it reached the endothermic peaks at 662 ºC (natural) and 676 ºC (calcined), with mass loss of approximately 6% and 3%, respectively, which were associated with the decarbonization process of the samples, by the decomposition of $CaCO_3$ present in the samples, mainly due to the cementitious material in its composition [63, 64].

The micrographs were used to investigate the morphology of the samples, as well as the microstructural changes as a function of the treatment performed. In this sense, it is possible to observe the existence of irregular plates of different sizes and the presence of non-uniform aggregates for the two samples, but it was also noted that they had similar morphologies [65], as observed in Fig. 5. In calcined residue samples, small agglomerations were seen between particles, which affects the specific surface area of the samples directly [65, 66] that was proven by physical adsorption of N_2, since the application of temperature causes coalescence between the grains, implying the reduction of the surface area and pore volume of the samples, because, at the same time that the material dehydration occurs, structural changes are also perceived.

Point of zero charge (Fig. 6) is a important parameter, widely used to measure the potential charge interaction between the adsorbent and the adsorbate. In this sense, pH_{pzc} corresponds to the range in which the pH of the solution remains constant, so that pH_i-pH_f is equal to zero. Thus, if the pH is less than pH_{pzc}, the surface charge of the adsorbent is positive, while for values higher than the pH_{pzc} the surface charge of the material is negative. The result is expressed through a graph of ΔpH (pH_i-pH_f) as a function of the pH_i [67]. The pH_{pzc} values estimated graphically for the samples were 10.0 (natural) and 10.9 (calcined). This indicated that at pH above pH_{pzc}, the surface of the materials will present a higher concentration of negative charges, then it will adsorb cationic dyes with greater efficiency [67].

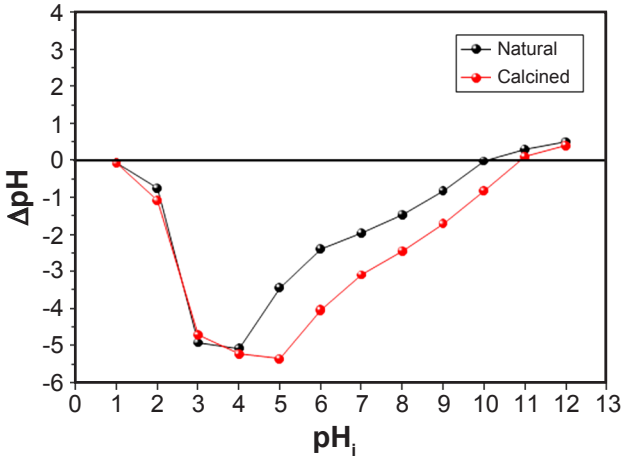

Figure 6: Graph of ΔpH (pH_i-pH_f) as a function of the pH_i for determination of point of zero charge (pH_{pzc}) of the natural and calcined samples.

Adsorption experiments

Effect of adsorbent dosage: the effect of adsorbent dosage on the adsorption of methylene blue dye for natural and calcined samples is shown in Fig. 7. It was noted that the adsorption coefficient was different for the calcined sample in relation to the natural sample. It was observed that the highest adsorption capacity refered to the calcined sample, which obtained a result of 12.86 $mg.g^{-1}$, equivalent to 6.95% of dye removal, for 10 mg of calcined residue mass, while the natural sample adsorbed 2.72 $mg.g^{-1}$, equivalent to 1.31%, also for a mass of 10 mg, showing that the results were better for the calcined sample (10 mg). Therefore, for the calcined sample, the adsorption capacity tended to decrease with the reduction of adsorbate/adsorbent ratio, making the system that contained the lowest amount of adsorbent mass presented a better performance. On the other hand, the increase in the mass of the adsorbent may also favor the formation of agglomerates, making difficult the adsorption [68], therefore, observing these factors and also in order to standardize the masses to favor the comparison of the results, the mass of the two samples was fixed at 10 mg.

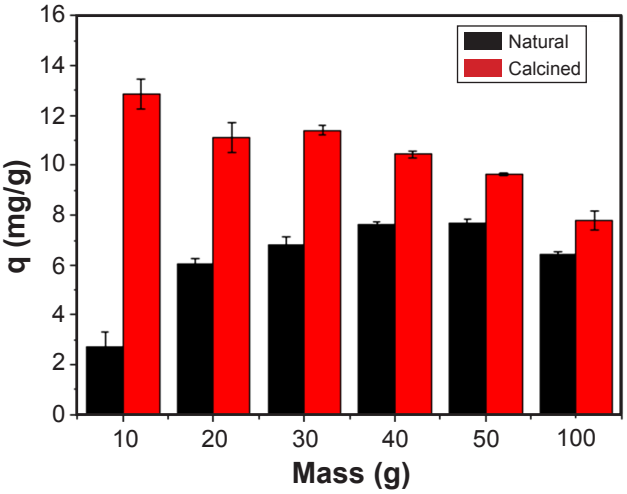

Figure 7: Effect of dosage for the adsorption of methylene blue dye on natural and calcined samples.

Effect of pH: methylene blue dye produces molecular cations in aqueous solution, and adsorption is mainly influenced by the superficial charge of the adsorbent [69]. Therefore, as shown by the point of zero charge (pH_{pzc}), the surfaces of the two samples had varied interaction ranges. However, for both samples of natural and calcined residues the best pH of adsorption was pH 12, with adsorption capacity of 22.69 $mg.g^{-1}$ (natural) and 79.74 $mg.g^{-1}$ (calcined), as can be seen in Fig. 8. As shown by the pH_{pzc}, adsorbent surfaces had negative charge density at pH above 10.0 (natural) and 10.9 (calcined), so the adsorption of methylene blue dye on the surface of the residues is influenced mainly by the surface charge of the adsorbents; so as, the pH of the solution increases, the number of adsorbent sites with negative charge also increases, due to the deprotonation of silanol groups, present in silica, and these factors improve

the electrostatic interaction between the methylene blue dye, that is a cationic, and the surfaces of materials with high pH values. For this reason, pH 12 performed better. On the other hand, acid pH reflects the presence of ions H^+ in excess that start to compete with dye cations for the adsorption sites [70, 71]. In relation to the pH 10 and 11 values, a slight decrease in dye adsorption was observed rather than the expected increase, which may be associated with another adsorption mode [72]. Based on these results, it can be considered the adsorption mechanism of methylene blue dye on the CDW occurred through electrostatic interactions and ion exchange, because the CDW surface had negative charge density that interacted with the cationic dye, facilitating the adsorption, while it was benefited from porous structure and the presence of functional groups on the surface of the ceramic matrix.

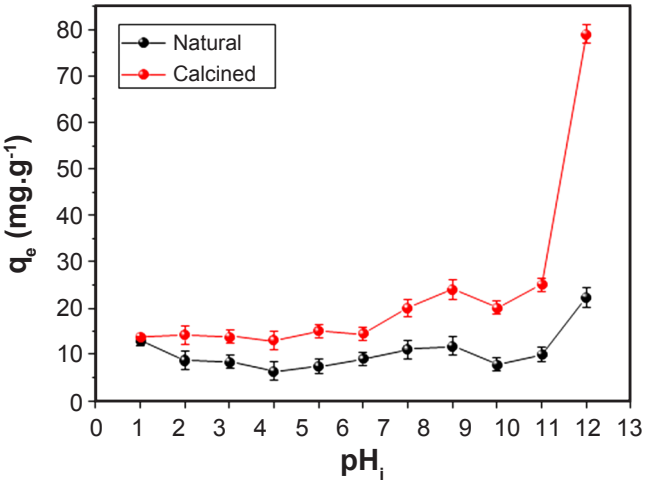

Figure 8: Effect of pH for the adsorption of methylene blue dye on natural and calcined samples.

Effect of contact time: regarding the contact effect, Fig. 9 presents the adsorption kinetics of methylene blue dye for natural and calcined materials. It was observed that the equilibrium time in the described conditions was approximately 840 min for both samples, and the experimental adsorption data for natural and calcined were approximately 22.47 and 79.48 mg.g^{-1}, respectively, similar to those observed in the effect of pH (22.69 mg.g^{-1} for natural and 79.74 mg.g^{-1} for calcined), considered satisfactory, comparing to results presented by other studies [73, 74] for alternative materials applied to adsorption. It was also observed that the adsorbed amounts increased with the passage of contact time until reaching the equilibrium

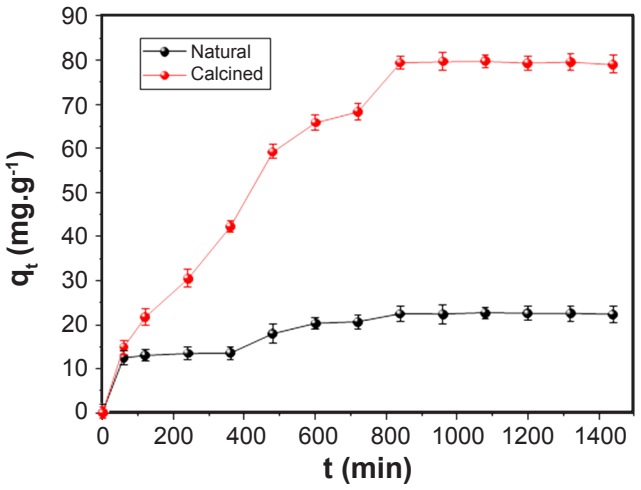

Figure 9: Effect of contact time for the adsorption of methylene blue dye on natural and calcined samples. Conditions: mass=10 mg; T=25 ºC; agitation speed=180 rpm; pH=12.

due to the diffusion of the dye in the medium, increasing the adsorption efficiency of the species due to the thermal energy of the system [75].

In order to understand how the kinetic behavior of dye adsorption occurs in the materials under study, the experimental data obtained were applied to the kinetic models of pseudo-first-order, pseudo-second-order and Elovich, according to Table III. Therefore, the values of determination coefficients (R^2) obtained from the linear adjustments of the equations related to the kinetic models presented were compared. It was possible to observe through the results that the experimental data were better adjusted to the pseudo-second-order model, which determines chemisorption as the main stage of the adsorptive process. Thus, it can be confirmed that this model is the one that best describes the adsorption of methylene blue dye for both adsorbents, by the best perceived linearity through the determination coefficient (R^2 >0.98) of the samples, as well as the greater approximation between the $q_{e,exp}$ and $q_{e,cal}$, because this model is most frequently cited in the literature for the adsorption of dyes using adsorbents of this nature [76, 77]. Fig. 10 presents the linear adjustments in relation to the three kinetic models considered, showing that the best adjustment was for pseudo-second-order.

Effect of temperature and dye concentration: Fig. 11 represents the adsorption isotherms for the methylene blue dye, in which the concentration and temperature parameters

Table III - Kinetic model parameters for the adsorption of methylene blue dye on natural and calcined residues.

Adsorbent	Pseudo-first-order			Pseudo-second-order				Elovich		
	k_1 (min^{-1})	$q_{e,cal}$ (mg.g^{-1})	R^2	k_2 (g.mg^{-1}.min^{-1})	$q_{e,cal}$ (mg g^{-1})	h (mg.g^{-1}.min^{-1})	R^2	α (mg.g^{-1}.min^{-1})	β (g.mg^{-1})	R^2
Natural	0.0034	16.1087	0.8432	2.6662x10^{-4}	25.1446	0.1686	0.9866	0.8980	0.2513	0.8714
Calcined	0.0051	114.6610	0.6720	2.3117x10^{-5}	106.7236	0.2633	0.9802	0.5852	0.0423	0.9616

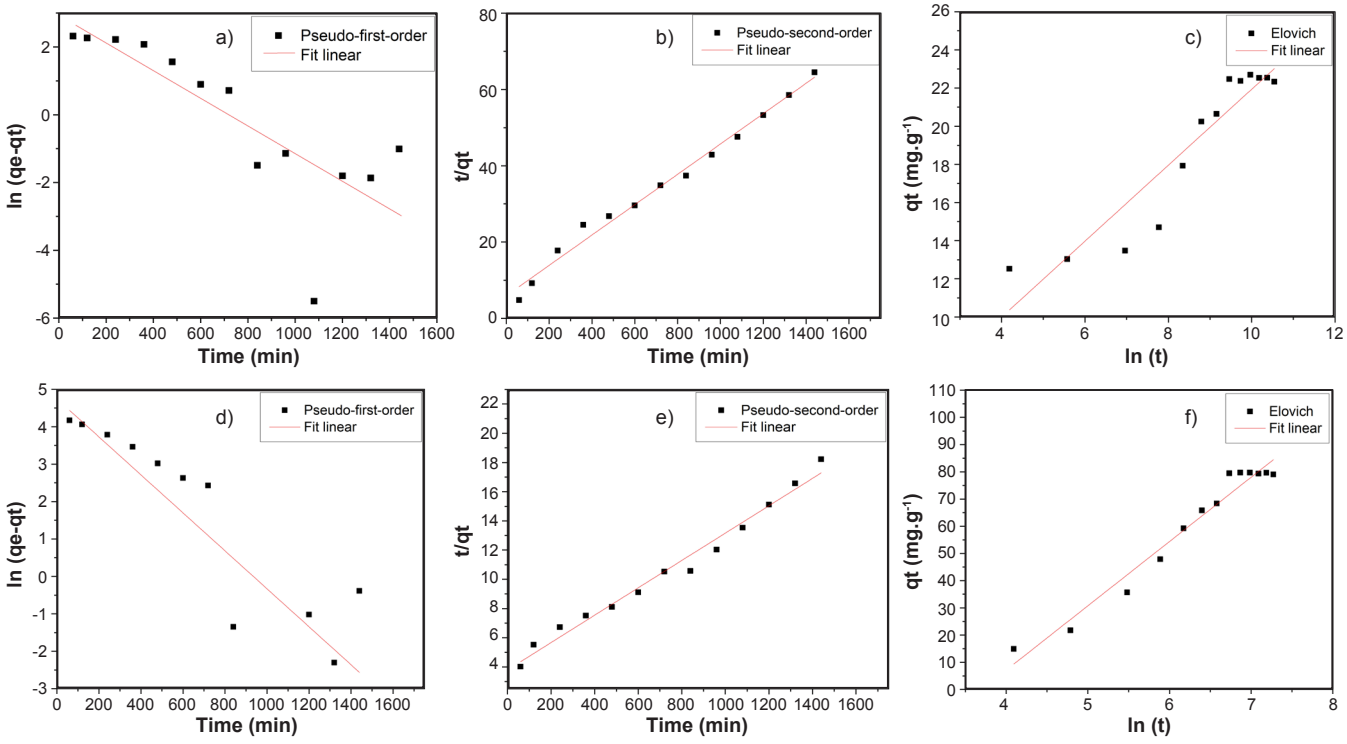

Figure 10: Linear fitting of the influence of time (t) on adsorption for the methylene blue by natural (a,b,c) and calcined (d,e,f) residues. Conditions: mass=10 mg; T=25 ºC; agitation speed=180 rpm; pH=12.

of the system were evaluated. The maximum adsorption capacity for natural residue at 25, 35 and 45 °C was 35.9, 60.45 and 112.23 mg.g^{-1}, respectively, and, for calcined residue, at the same temperatures, it was obtained 197.3, 253.5 and 418.6 mg.g^{-1}, respectively. Thus, the adsorption process was endothermic for both samples, because the adsorption coefficient was directly proportional to the temperature increase. Tables IV and V show the data and parameters of the adsorption isotherms of methylene blue dye in relation to natural and calcined residues, as well as their respective adaptations to the models described above, the correlation coefficients and temperatures studied. Fig. 12 presents linear adjustments to the Langmuir, Freundlich and Temkin models for both samples.

It is observed that the best fit to the experimental data was for the Langmuir isotherm model for both samples, with a determination coefficient varying between $0.9721 \leq R^2 \leq 0.9910$ for the natural sample and between $0.9608 \leq R^2 \leq 0.9827$ for calcined sample. When comparing the theoretical adsorption values (q_{max}) with those obtained experimentally, it was observed that the Langmuir model provided better parameters than the Freundlich and Temkin models. Furthermore, it was seen graphically (Fig. 12) that the best fit was for the Langmuir isotherm model for

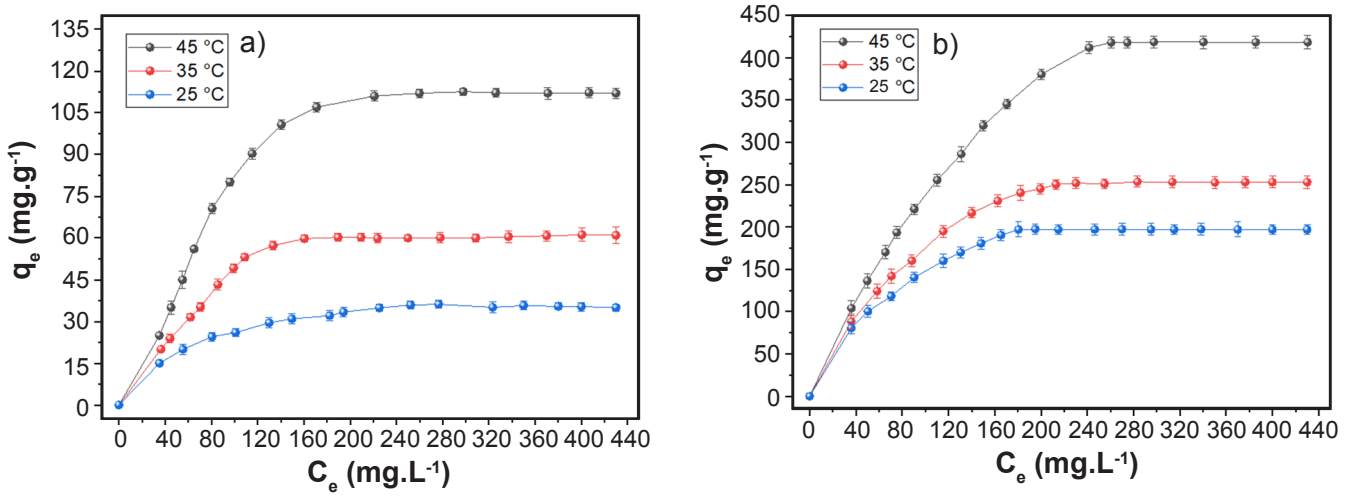

Figure 11: Adsorption isotherms of methylene blue dye of natural (a) and calcined (b) residues.

Table IV - Isotherm model parameters for the adsorption of methylene blue dye on natural sample.

Temperature (K)	Langmuir				Freundlich			Temkin		
	$q_{máx}$ (mg.g^{-1})	K_L (L.mg^{-1})	R_L	R^2	n_f	K_f (L.g^{-1})	R^2	A_T (L.mg^{-1})	b_T (J.mol^{-1})	R^2
298	41.8410	0.0178	0.1824	0.9910	3.1790	5.9648	0.8543	0.1993	284.0399	0.9009
308	73.9098	0.0156	0.2851	0.9721	2.3511	5.7766	0.7959	0.1260	147.3614	0.8477
318	138.5041	0.0127	0.2626	0.9824	1.9583	6.3715	0.8926	0.1089	82.1100	0.9466

Table V - Isotherm model parameters for the adsorption of methylene blue dye on calcined sample.

Temperature (K)	Langmuir				Freundlich			Temkin		
	$q_{máx}$ (mg.g^{-1})	K_L (L.mg^{-1})	R_L	R^2	n_f	K_f (L.g^{-1})	R^2	A_T (L.mg^{-1})	b_T (J.mol^{-1})	R^2
298	240.9639	0.0170	0.2460	0.9827	2.5068	22.308	0.8749	0.1364	43.9861	0.9015
308	319.4888	0.0131	0.2775	0.9810	2.2581	21.612	0.8960	0.1007	33.4042	0.9286
318	613.4970	0.0066	0.3866	0.9608	1.7218	15.466	0.9336	0.0533	17.7975	0.9607

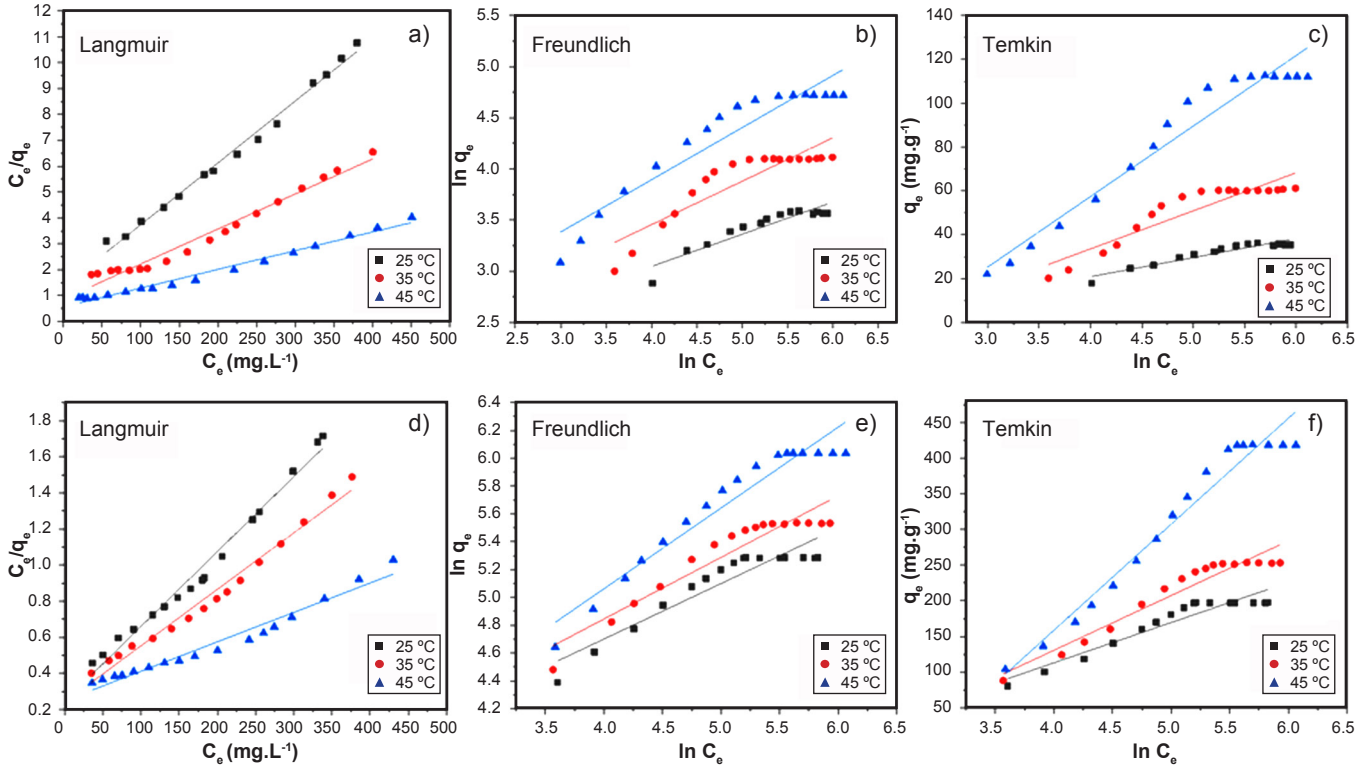

Figure 12: Linear fitting of the adsorption isotherms for the methylene blue by natural (a,b,c) and calcined (d,e,f) samples.

both adsorbents, which considers that sorption occurs in monolayer, that is, in specific homogeneous sites of the adsorbent [78]. The value of the separation factor or equilibrium parameter (R_L), priceless for Langmuir model, showed that the natural and calcined samples were in the range in which the adsorption mechanism is considered favorable, in view of the three temperatures studied, because ($0<R_L<1$), thus, it is suggested that both samples had a considerable affinity for the adsorbent matrix [79]. Moreover, it is important to highlight that desorption and regeneration studies of the adsorbents are mechanisms very important to promote the reutilization, sustainability, economy, and optimization of the adsorption process, contributing to the better management of the resources and consequently environment protection. In this sense, to optimize the efficiency of the cycles of regeneration, many methods can be used, such as steam and chemical regeneration [80] that will be considered in a future work.

Thermodynamic parameters for the adsorption: adsorption data of methylene blue dye by natural and

Table VI - Thermodynamic parameters of the adsorption of methylene blue dye to natural and calcined sample.

	Temperature (ºC)	ΔG (kJ.mol^{-1})	ΔH (kJ.mol^{-1})	ΔS (J.mol^{-1}.K^{-1})
Natural	25	4.5810	49.9527	152.2540
	35	3.0585		
	45	1.5359		
Calcined	25	-0.1171	15.0762	50.9842
	35	-0.6270		
	45	-1.1368		

calcined samples obtained experimentally were adjusted to the equations and the thermodynamic behavior of adsorption were measured by enthalpy (ΔH), entropy (ΔS) and Gibbs free energy (ΔG) variations, according to the Tables VI. It was observed that the Gibbs free energy (ΔG) of the natural sample showed positive values, indicating that the process was not spontaneous for any of the temperatures studied. Nevertheless, ΔG tended to decrease due to the increase in temperature, indicating that the process was favored at high temperatures, which implies saying that ΔG will obtain negative values with the increase in temperature, making the process spontaneous. Differently, the calcined sample showed negative values for ΔG, evidencing that the process was thermodynamically spontaneous and favorable. It was also observed that the value of ΔG tended to decrease with the increase in temperature, indicating a clear tendency that the process was favored with the increase in temperature. The variation of enthalpy (ΔH) was positive for both samples, indicating the endothermic nature of the adsorption. In this case, higher temperatures promote more spontaneous adsorptions. The value of entropy variation (ΔS) positive showed that there was an increase in the disorder in the solid/liquid interface during the adsorption process, also indicating the increase in the degree of freedom of the adsorbed species [81-84].

CONCLUSIONS

A proposal for the use of construction and demolition wastes as alternative materials for adsorption of methylene blue dye in aqueous medium was presented. Two samples were used, the residue in natural and calcined states, both characterized by XRD, FRX, FTIR, TG/DTG, BET and SEM. It was observed, through the kinetic study, that the equilibrium time was 840 min for both samples, and the experimental adsorption data were approximately 22.69 mg.g^{-1} (natural) and 79.74 mg.g^{-1} (calcined), better adjusting to the pseudo-second-order model, with both determination coefficient R^2 >0.980. The adsorption results for the concentration and temperature effect were 35.9, 60.45 and 112.23 mg.g^{-1} (natural) and 197.3, 253.5 and 418.6 mg.g^{-1} (calcined) for the temperatures of 25, 35 and 45 °C, respectively. The experimental data were better adjusted to the Langmuir model, with R^2 >0.960 and the equilibrium parameter (R_L) favorable for both samples. Thermodynamic analysis showed that adsorption is spontaneous and feasible for calcined residue and not spontaneous for natural residue at the studied temperatures, although, for both adsorbents, the process was favored with increasing temperature, indicating the endothermic nature of the two systems. However, considering the results presented, it was observed that despite the calcined sample presented better results than the natural sample, the energy of calcination at 700 ºC could make the process more expensive, and, thinking on the reduction of the costs, the natural sample can be more advantageous. In view of this, it can be concluded that construction and demolition waste can be used in the process of adsorption of methylene blue dye in aqueous medium since this material presented good adsorption parameters, representing a promising alternative in the water purification process.

REFERENCES

[1] Salleh SZ, Kechik AA, Yusoff AH, Taib MAA, Nor MM, Mohamad M, et al. Recycling food, agricultural, and industrial wastes as pore-forming agents for sustainable porous ceramic production: A review. J Clean Prod. 2021;**306**:127264.

[2] Ranjbari M, Shams Esfandabadi Z, Zanetti MC, Scagnelli SD, Siebers PO, Aghbashlo M, et al. Three pillars of sustainability in the wake of COVID-19: A systematic review and future research agenda for sustainable development. J Clean Prod. 2021;**297**.

[3] Andriamanantena M, Razafimbelo FF, Raonizafinimanana B, Cardon D, Danthu P, Lebeau J, et al. Alternative sources of red dyes with high stability and antimicrobial properties: Towards an ecological and sustainable approach for five plant species from Madagascar. J Clean Prod. 2021;**303**:126979.

[4] Barbosa A, Silva C, Mauricio R, Andrade DF, Freire FB, Nagalli A, et al. Análise da utilização de cerâmica vermelha como adsorvente na remoção do corante têxtil Direct Blue de uma solução aquosa. Revista Materia. 2017;**22**.

[5] Leal TW, Lourenço LA, Scheibe AS, Souza SMAGU, Souza AAU. Textile wastewater treatment using low-cost adsorbent aiming the water reuse in dyeing process. J Environ Chem Eng. 2018;**6**:2705–2712.

[6] Guaratini CCI, Zanoni MVB. Corantes têxteis. Quim Nova. 2000;**23**:71–78.

[7] Zanella G, Scharf M, Vieira GA, Peralta-Zamora P. Tratamento de banhos de tingimento têxtil por processos

foto-Fenton e avaliação da potencialidade de reuso. Quim Nova. 2010;**33**:1039–1043.
[8] Abdelrahman EA, Hegazey RM, El-Azabawy RE. Efficient removal of methylene blue dye from aqueous media using Fe/Si, Cr/Si, Ni/Si, and Zn/Si amorphous novel adsorbents. J Mater Res Technol. 2019;**8**:5301–5313.
[9] Lima JP, Alvarenga G, Goszczynski ACF, Rosa GR, Lopes TJ. Batch adsorption of methylene blue dye using Enterolobium contortisiliquum as bioadsorbent: Experimental, mathematical modeling and simulation. J Ind Eng Chem. 2020;**91**:362–371.
[10] Jawad AH, Abdulhameed AS. Mesoporous Iraqi red kaolin clay as an efficient adsorbent for methylene blue dye: Adsorption kinetic, isotherm and mechanism study. Surf Interfaces. 2020;**18**.
[11] Wekoye JN, Wanyonyi WC, Wangila PT, Tonui MK. Kinetic and equilibrium studies of Congo red dye adsorption on cabbage waste powder. Environ Chem Ecotoxicol. 2020;**2**:24–31.
[12] Kallel F, Chaari F, Bouaziz F, Bettaieb F, Ghorbel R, Chaabouni SE. Sorption and desorption characteristics for the removal of a toxic dye, methylene blue from aqueous solution by a low cost agricultural by-product. J Mol Liq. 2016;**219**:279–288.
[13] Almeida CRG, Franco J, Tavares JM. Influência do tipo de argila no processo de solidificação/estabilização de lodo têxtil. Ceramica. 2015;**61**:137–144.
[14] Vasques AR, Souza SMAGU, Weissenberg L, Souza AAU, Valle JAB. Adsorção dos corantes RO16, RR2 e RR141 utilizando lodo residual da indústria têxtil. Eng Sanit Ambient. 2011;**16**:245–252.
[15] Omo-okoro PN, Daso AP, Okonkwo JO. A review of the application of agricultural wastes as precursor materials for the adsorption of per- and polyfluoroalkyl substances: A focus on current approaches and methodologies. Environ Technol Innov. 2018;**9**:100–114.
[16] Pereira VC, Nascimento PMKB, Nunes CN, Gimenes ML, Cordeiro PHY, Lima LS, et al. Removal of Alprazolam in Contaminated Waters: Evaluation of Alternative Adsorbents. Rev Virtual Quim. 2019;**11**:893–908.
[17] Favaretto P, Hidalgo GEN, Sampaio CH, Silva RA, Lermen RT. Characterization and Use of Construction and Demolition Waste from South of Brazil in the Production of Foamed Concrete Blocks. Appl Sci. 2017;**7**.
[18] Islam R, Nazifa TH, Yuniarto A, Shanawaz Uddin ASM, Salmiati S, Shahid S. An empirical study of construction and demolition waste generation and implication of recycling. Waste Manag. 2019;**95**:10–21.
[19] Akhtar A, Sarmah AK. Construction and demolition waste generation and properties of recycled aggregate concrete: A global perspective. J Clean Prod. 2018;**186**:262–281.
[20] De Brito J, Silva R. Current status on the use of recycled aggregates in concrete: Where do we go from here? RILEM Tech Lett. 2016;**1**:1.
[21] Azevedo GOD, Kiperstok A, Moraes LRS. Resíduos da construção civil em Salvador: os caminhos para uma gestão sustentável. Eng Sanit Ambient. 2006;**11**:65–72.
[22] Iodice S, Garbarino E, Cerreta M, Tonini D. Sustainability assessment of Construction and Demolition Waste management applied to an Italian case. Waste Manag. 2021;**128**:83–98.
[23] Qiao L, Tang Y, Li Y, Liu M, Yuan X, Wang Q, et al. Life cycle assessment of three typical recycled products from construction and demolition waste. J Clean Prod. 2022;**376**:134139.
[24] Borghi G, Pantini S, Rigamonti L. Life cycle assessment of non-hazardous Construction and Demolition Waste (CDW) management in Lombardy Region (Italy). J Clean Prod. 2018;**184**:815–825.
[25] Rosado LP, Vitale P, Penteado CSG, Arena U. Life cycle assessment of natural and mixed recycled aggregate production in Brazil. J Clean Prod. 2017;**151**:634–642.
[26] Fernandes A, Amorim J. Colégio de Ciências Exatas, Tecnológicas e Multidisciplinar: Atualização de Área. Caderno de Graduação - Ciências Exatas e Tecnológicas - UNIT. 2014;**2**:79–104.
[27] Cordeiro GC, Désir JM. Potencial de argila caulinítica de Campos dos Goytacazes, RJ, na produção de pozolana para concreto de alta resistência. Ceramica. 2010;**56**:71–76.
[28] Oliveira FM, Coelho LM, Melo EI. Memória e metapoesia em João Cabral de Melo Neto e Carlos de Oliveira. Rev Mater. 2018;**23**.
[29] Hatiya NA, Reshad AS, Negie ZW. Chemical Modification of Neem (Azadirachta indica) Biomass as Bioadsorbent for Removal of Pb^{2+} Ion from Aqueous Waste Water. Adsorpt Sci Technol. 2022;**2022**:1–18.
[30] Stavrinou A, Theodoropoulou MA, Aggelopoulos CA, Tsakiroglou CD. Removal of Phenanthrene from wastewater with low-cost adsorbents. IOP Conf Ser Earth Environ Sci. 2022;**1123**:012081.
[31] Feddane S, Oukebdane K, Didi MA, Didi A, Amara A, Larabi O. Removal of textile dye Bemacid Red from water using Casuarina equisetifolia needles: kinetic and thermodynamic modeling. Desalination Water Treat. 2023;**289**:248–257.
[32] Sousa HR, Silva LS, Sousa PAA, Sousa RRM, Fonseca MG, Osajima JA, et al. Evaluation of methylene blue removal by plasma activated palygorskites. J Mater Res Technol. 2019;**8**:1–11.
[33] Khezami L, Capart R. Removal of chromium(VI) from aqueous solution by activated carbons: Kinetic and equilibrium studies. J Hazard Mater. 2005;**123**:223–231.
[34] Kumar D, Gaur JP. Corrigendum to "Engineering interventions in enzyme production: Lab to industrial scale" [Bioresour. Technol. 326 (2021) 124771]. Bioresour Technol. 2011;**102**:633–640.
[35] Kim JR, Santiano B, Kim H, Kan E. Heterogeneous Oxidation of Methylene Blue with Surface-Modified Iron-Amended Activated Carbon. Am J Anal Chem. 2013;**4**:115–122.
[36] Chan LS, Cheung WH, McKay G. Adsorption of acid dyes by bamboo derived activated carbon. Desalination. 2008;**218**:304–312.

[37] Akolo SA, Kovo AS. Comparative Study of Adsorption of Copper Ion onto Locally Developed and Commercial Chitosan. J Encapsulation Adsorpt Sci. 2015;**5**:21–37.
[38] Chen H, Wang A. Kinetic and isothermal studies of lead ion adsorption onto palygorskite clay. J Colloid Interface Sci. 2007;**307**:309–316.
[39] Arfaoui S, Frini-Srasra N, Srasra E. Modelling of the adsorption of the chromium ion by modified clays. Desalination. 2008;**222**:474–481.
[40] Maroneze MM, Zepka LQ, Vieira JG, Queiroz MI, Jacob-Lopes E. A tecnologia de remoção de fósforo: gerenciamento do elemento em resíduos industriais. Rev Ambient Agua. 2014;**9**:445–458.
[41] Silva W, Oliveira S. Physicochemical characterization and antibacterial activity of Brazilian artisanal milk kefir. Sci Plena. 2012;**8**:1–9.
[42] Dotto G, Vieira M, Gonçalves J, Pinto L. Remoção dos corantes azul brilhante, amarelo crepúsculo e amarelo tartrazina de soluções aquosas utilizando carvão ativado, terra ativada, terra diatomácea, quitina e quitosana: estudos de equilíbrio e termodinâmica. Quim Nova. 2011;**34**:1193–1199.
[43] Sá ML, Nobre FX, Matos JME, Santos MRMC. Remoção do alaranjado de metila em meio aquoso por microcristais de h-MoO_3 obtidos pelo método micro-ondas hidrotérmico. Ceramica. 2020;**66**:197–207.
[44] Cardoso NF, Lima EC, Royer B, Bach MV, Dotto GL, Pinto LAA, et al. Comparison of Spirulina platensis microalgae and commercial activated carbon as adsorbents for the removal of Reactive Red 120 dye from aqueous effluents. J Hazard Mater. 2012;**241–242**:146–153.
[45] Machado FM, Bergmann CP, Fernandes THM, Lima EC, Royer B, Calvete T, et al. Adsorption of Reactive Red M-2BE dye from water solutions by multi-walled carbon nanotubes and activated carbon. J Hazard Mater. 2011;**192**:1122–1131.
[46] Calvete T, Lima EC, Cardoso NF, Dias SLP, Pavan FA. Application of carbon adsorbents prepared from the Brazilian pine-fruit-shell for the removal of Procion Red MX 3B from aqueous solution—Kinetic, equilibrium, and thermodynamic studies. Chem Eng J. 2009;**155**:627–636.
[47] Tran HN, You SJ, Chao HP. Thermodynamic parameters of cadmium adsorption onto orange peel calculated from various methods: A comparison study. J Environ Chem Eng. 2016;**4**:2671–2682.
[48] Prasanphan S, Hemra K, Wannagon A, Kobayashi T, Onutai S, Jiemsirilers S. 29Si and 27Al NMR study of the structural transformation of calcined kaolin residue-based geopolymer using low alkali activator content for sustainable construction materials. J Build Eng. 2023;**70**:106332.
[49] Ghyati S, Kassou S, El Jai M, El Kinani EH, Benhamou M. Investigation of PEG4000/Natural clay-based hybrids: Elaboration, characterization and theory. Mater Chem Phys. 2020;**239**:121993.
[50] Santos GR, Salvetti AR, Cabrelon MD, Morelli MR. Synthetic flux as a whitening agent for ceramic tiles. J Alloys Compd. 2014;**615**:S459–S461.
[51] Azevedo ARG, França BR, Alexandre J, Marvila MT, Zanelato EB, Xavier GC. Influence of sintering temperature of a ceramic substrate in mortar adhesion for civil construction. J Build Eng. 2018;**19**:342–348.
[52] Vigneron TQG, Vieira CMF, Delaqua GCG, Vernilli Júnior F, Neto ÂC. Incorporation of mold flux waste in red ceramic. J Mater Res Technol. 2019;**8**:5707–5715.
[53] De Faria JS, Manhães RDST, Da Luz FS, Monteiro SN, Vieira CMF. Incorporation of unserviceable tire waste in red ceramic. J Mater Res Technol. 2019;**8**:6041–6050.
[54] España VAA, Sarkar B, Biswas B, Rusmin R, Naidu R. Environmental applications of thermally modified and acid activated clay minerals: Current status of the art. Environ Technol Innov. 2019;**13**:383–397.
[55] Yan S, Huo W, Yang J, Zhang X, Wang Q, Wang L, et al. Green synthesis and influence of calcined temperature on the formation of novel porous diatomite microspheres for efficient adsorption of dyes. Powder Technol. 2018;**329**:260–269.
[56] Ribeiro LS, Babisk MP, Prado US, Monteiro SN, Vieira CMF. Incorporation of in Natura and Calcined Red Muds into Clay Ceramic. Mater Res. 2015;**18**:279–282.
[57] Jelić I, Šljivić-Ivanović M, Dimović S, Antonijević D, Jović M, Mirković M, et al. The applicability of construction and demolition waste components for radionuclide sorption. J Clean Prod. 2018;**171**:322–332.
[58] Andrade JJO, Possan E, Squiavon JZ, Ortolan TLP. Evaluation of mechanical properties and carbonation of mortars produced with construction and demolition waste. Constr Build Mater. 2018;**161**:70–83.
[59] Komnitsas K, Zaharaki D, Vlachou A, Bartzas G, Galetakis M. Effect of synthesis parameters on the quality of construction and demolition wastes (CDW) geopolymers. Adv Powder Technol. 2015;**26**:368–376.
[60] Komnitsas K. Co-valorization of marine sediments and construction & demolition wastes through alkali activation. J Environ Chem Eng. 2016;**4**:4661–4669.
[61] Cristelo N, Fernández-Jiménez A, Vieira C, Miranda T, Palomo Á. Stabilisation of construction and demolition waste with a high fines content using alkali activated fly ash. Constr Build Mater. 2018;**170**:26–39.
[62] Zhang Y, Wang W, Zhang J, Liu P, Wang A. Preparation and Mechanism Study of Green Cyanamide Calcium. Chem Eng J. 2015;**262**:390–398.
[63] Almeida Neto AF, Vieira MGA, Silva MGC. Avaliação dos Níveis de Curto-Circuito e Perda de Sensibilidade em um Alimentador de Rede de Distribuição na Presença de Geração Distribuída. VI Conferência Brasileira Sobre Temas de Tratamento Térmico. 2012;**312–323**.
[64] Gonçalves JP, Toledo Filho RD, Fairbairn EMR. Influência da substituição parcial de cimento por cinza ultrafina da casca de arroz com elevado teor de carbono nas propriedades do concreto. Ambient Constr. 2006;**6**:83–94.
[65] Vilar WCT, Brito ALF, Laborde HM, Laborde M, Rodrigues MGF, Ferreira HS. The Abbe Laborde on the Immaculate Conception. Rev Eletron Mater Process. 2009;**3**:39–47.

[66] He C, Makovicky E, Osbæck B. Thermal treatment and pozzolanic activity of sepiolite. Appl Clay Sci. 2000;**17**:141–161.
[67] Guida IIS, Falcão SS. Removal of Crystal Violet Textile Using Clay Maranhese of High Mounts as Adsorvent. Rev Virtual Quim. 2018;**10**:1087–1099.
[68] Silva LS, Ferreira FJL, Silva MS, Citó AMGL, Meneguin AB, Sábio RM, et al. Potential of amino-functionalized cellulose as an alternative sorbent intended to remove anionic dyes from aqueous solutions. Int J Biol Macromol. 2018;**116**:1282–1295.
[69] Özdemir Y, Doğan M, Alkan M. Adsorption of cationic dyes from aqueous solutions by sepiolite. Microporous Mesoporous Mater. 2006;**96**:419–427.
[70] Almeida CAP, Debacher NA, Downs AJ, Cottet L, Mello CAD. Removal of methylene blue from colored effluents by adsorption on montmorillonite clay. J Colloid Interface Sci. 2009;**332**:46–53.
[71] Hamdaoui O. Batch study of liquid-phase adsorption of methylene blue using cedar sawdust and crushed brick. J Hazard Mater. 2006;**135**:264–273.
[72] Garg VK, Gupta R, Yadav AB, Kumar R. Dye removal from aqueous solution by adsorption on treated sawdust. Bioresour Technol. 2003;**89**:121–124.
[73] Rafatullah M, Sulaiman O, Hashim R, Ahmad A. Adsorption of methylene blue on low-cost adsorbents: A review. J Hazard Mater. 2010;**177**:70–80.
[74] Chahm T, Martins BA, Rodrigues CA. Adsorption of methylene blue and crystal violet on low-cost adsorbent: waste fruits of Rapanea ferruginea (ethanol-treated and H_2SO_4-treated). Environ Earth Sci. 2018;**77**.
[75] Roulia M, Vassiliadis AA. Sorption characterization of a cationic dye retained by clays and perlite. Microporous Mesoporous Mater. 2008;**116**:732–740.
[76] Gürses A, Doğar Ç, Yalçin M, Açikyildiz M, Bayrak R, Karaca S. Investigation of agglomeration rates of two Turkish lignites. J Hazard Mater. 2006;**131**:217–228.
[77] Silva MP, Santos MSF, Santos MRMC, Santos LS Jr, Fonseca MG, Silva Filho EC. Natural Palygorskite as an Industrial Dye Remover in Single and Binary Systems. Mater Res. 2016;**19**:1232–1240.
[78] Paula LNR, Paula GM, Rodrigues MGF. Adsorption of reactive blue BF-5G dye on MCM-41 synthesized from Chocolate clay. Ceramica. 2020;**66**:269–276.
[79] Leandro-Silva E, Pipi ARF, Magdalena AG, Piacenti-Silva M. Remoção de Metais Usando Nanopartículas de Fe_3O_4-Quitosana para Aplicações Ambientais. Rev Mater. 2020;**25**:1–12.
[80] Gao R, Liu D, Huang Y, Li G. Preparation of diatomite-modified wood ceramics and the adsorption kinetics of tetracycline. Ceram Int. 2020;**46**:19799–19806.
[81] Kula I, Uğurlu M, Karaoğlu H, Çelik A. Adsorption of Cd(II) ions from aqueous solutions using activated carbon prepared from olive stone by $ZnCl_2$ activation. Bioresour Technol. 2008;**99**:492–501.
[82] Olivares-Marín M, Fernández-González C, Macías-García A, Gómez-Serrano V. Preparation of activated carbon from cherry stones by chemical activation with $ZnCl_2$. Appl Surf Sci. 2006;**252**:5967–5971.
[83] Murcia-Salvador A, Pellicer JA, Fortea MI, Gómez-López VM, Rodríguez-López MI, Núñez-Delicado E, et al. Adsorption of Direct Blue 78 Using Chitosan and Cyclodextrins as Adsorbents. Polym (Basel). 2019;**11**.
[84] S SE, Thinakaran N. Corrigendum to "Fly-ash scrubbing in a tapered bubble column scrubber" [Process Saf. Environ. Prot. 84 (2006) 54–62]. Process Saf Environ Prot. 2017;**106**:1–10.
(Rec. 02/02/2023, Rev. 05/07/2023, Ac. 04/11/2023) (AE: A. M. Segadães)